View metadata, citation and similar papers at core.ac.uk

brought to you by CORE

provided by IntechOpen

We are IntechOpen, the world's leading publisher of Open Access books Built by scientists, for scientists

4,800
Open access books available

122,000
International authors and editors

135M
Downloads

Our authors are among the

154
Countries delivered to

TOP 1%
most cited scientists

12.2%
Contributors from top 500 universities

CLARIVATE ANALYTICS BOOK CITATION INDEX INDEXED

WEB OF SCIENCE™

Selection of our books indexed in the Book Citation Index in Web of Science™ Core Collection (BKCI)

Interested in publishing with us?
Contact book.department@intechopen.com

Numbers displayed above are based on latest data collected.
For more information visit www.intechopen.com

Chapter 2

Alloy Development through Rapid Solidification for Soft Magnetic Application

Rajat K. Roy, Ashis K. Panda and Amitava Mitra

Additional information is available at the end of the chapter

http://dx.doi.org/0.5772/60772

Abstract

This chapter describes different rapidly solidified processing routes of soft magnetic alloys and their properties and applications in different areas. Section-2 explains the details of process mechanism. The functions of different alloying elements are discussed with the alloy design of soft magnetic alloys in section-3. The structure-property correlation is described in section-4. Section-5 highlights different types of rapidly solidified soft magnetic alloys, like high permeability alloys, high induction alloys, Fe-6.5 wt% Si steel and GMI alloys. In the last section-6, the applications of different types of soft magnetic alloys are mentioned.

Keywords: Rapid solidification, soft magnetism, alloy design, saturation induction, Fe-6.5 wt% Si steel, GMI alloys

1. Introduction

In recent years, amorphous and nanostructured soft magnetic alloys have gained considerable interest owing to their superior properties. Consequently, it catered to a broad area of applications such as transformer cores, magnetic field sensors, sensors for non-destructive evaluation of materials, motors, electric vehicles, etc. The bulk use of rapidly solidified iron-based magnetic materials is in distribution transformers due to its low core loss as compared to cold rolled grain orient (CRGO) Si steel. However, the use of amorphous alloy is limited only to low power transformers as the saturation induction of such alloy is low (~1.6T) as compared to CRGO Si steel (~ 2.1T). To overcome this problem the current trend is to work on

INTECH
open science | open minds

© 2015 The Author(s). Licensee InTech. This chapter is distributed under the terms of the Creative Commons Attribution License (http://creativecommons.org/licenses/by/3.0), which permits unrestricted use, distribution, and reproduction in any medium, provided the original work is properly cited.

high induction alloy so that the materials can be used for high frequency power transformers. Beside the distribution transformer, the high permeability amorphous or nanostructured magnetic alloys are used in switched mode power supply, switchgear, etc. In nanostructured alloys or nanocomposites which typically comprise nanocrystallites dispersed in amorphous matrix, the magnetic properties are controlled by the exchange of magnetic coupling between nanocrystallites through intergranular amorphous matrix. In these nanostructured materials, the extrinsic properties like coercivity and permeability are controlled through crystallite size and their distribution, whereas the intrinsic properties, like saturation magnetic induction (B_S) and Curie temperatures (T_C), are the functions of alloy chemistry of amorphous and nanocrystallite phases. The ultimate advancement of alloys is determined by the optimization of these intrinsic and extrinsic properties. Therefore, both designing of alloy composition and processing of alloys are equivalently important for attaining the ultimate goal of applications. In this chapter, the processing of different soft magnetic alloys through rapid solidification has been discussed, and the alloys are categorized according to their properties and applications.

2. Rapid solidification processing routes

2.1. Melt spinning technique

Amongst different rapid solidification processing routes, melt spinning is the most common technique for yielding soft magnetic metallic ribbons in large quantity. Sometimes this technique is also described as chill block melt spinning (CBMS). Basically, the ribbons are synthesized as the stream of molten alloy from a quartz crucible is purged through argon gas pressure on a rapidly rotating wheel made from the metals like pure Cu, Cu-Be alloy and stainless steel (Fig. 1). As shown in Fig. 1, the ribbon is typically maintaining a contact of sticking distance ($d_{t1}<d_{t2}<d_{t3}$) with the wheel surface before flying out of the wheel surface by centrifugal force. The adhesion time of ribbon at wheel surface is important for the ribbon preparation and depends on the process parameters and alloys used. It is observed that sticking distance of $Fe_{40}Ni_{40}B_{20}$ is less than that of $Fe_{81.5}B_{14.5}Si_4$ amorphous alloy on the Cu wheel [1]. Moreover, the ribbon thickness is quite important for controlling the ribbon properties, which is basically controlled by the rotating wheel speed, ejection pressure, nozzle slot size and crucible-wheel gap.

Huang et al. described the ribbon thickness effect on the core loss and excitation for straight and toroidal samples [2]. The optimum ribbon thickness of 30 μm has been found the most suitable for low core loss as well as low excitation (Fig. 2). For thin ribbon (<30 μm), both straight and toroidal samples show similar core loss and excitation, but for thick ribbons (>30 μm), core loss and excitation in toroidal samples are higher than the other. The magnetic domain structure is also responsible for better soft magnetic properties for the ribbons having thickness 25–30 μm as in such cases magnetic domains become parallel to ribbon thickness, whereas the ribbon with lower and higher thickness than above leads to transverse domain structure.

http://dx.doi.org/0.5772/60772

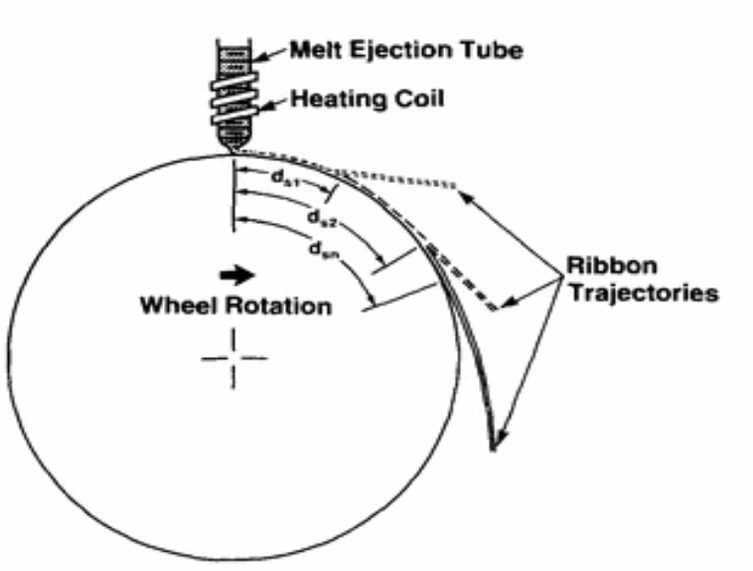

Figure 1. Schematic diagram showing ribbon preparation by single roller melt spinning technique and ribbon-wheel sticking distance at adhesion times t_1, t_2 and t_3 [1].

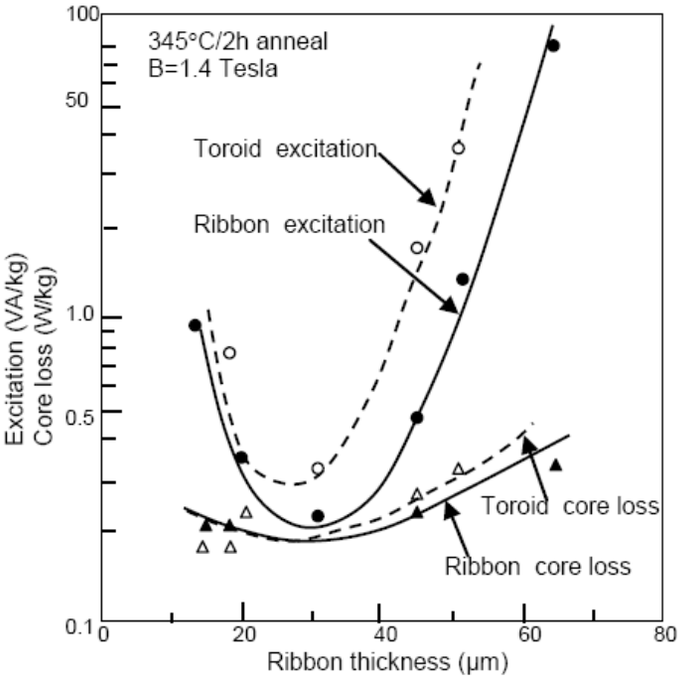

Figure 2. Ribbon thickness dependence of core loss and excitation for straight ribbons and 7.5 cm toroids, annealed at 345°C/2h, B = 1.4T [2].

2.2. In-rotating water quenching technique

Another way of preparing rapidly solidified materials is the processing of microwires (~100 μm diameter) by in-rotating water quenching technique. Unlike melt spinning, the amorphous

wire preparation through in-rotating water quenching technique involves rapid quenching of molten material inside the water of a rotating drum (Fig. 3). This processing route involves a stable melt impingement and minimum melt stream break into water surface and suitably carried along with the water's centrifugal velocity to acquire continuous wires. Therefore, in addition to the glass forming ability of alloys, the molten jet stability prior to quenching and high stability of water surface layer are prerequisite conditions for obtaining defect-free, continuous wires. Heyder et al. has reported that a non-viscous fluid jet may break into different steps like dropping, varicose breakup, sinuous breakup and atomization during the wire processing [3] and causes the powder formation in the quenching water. The increasing jet velocity can result in the rapid jet disintegration. The ratio between melt jet velocity (V_j) and cooling water velocity (V_w) is an important parameter to achieve straight wire. The ratio (V_j/V_w) has been found to be 0.9 for $Fe_{75}Si_{10}B_{15}$ metallic wires [3]. However, Olofinjana et al. have reported that the optimized ratio is in the range of 1.14–1.20 for the same aforementioned alloy and 1.16–1.18 for $Fe_{77.5}Si_{7.5}B_{15}$ alloy for continuous wire formation [4]. Therefore, a little difference in alloy composition and processing route may change the optimum ratio for achieving continuous wires. Additionally, other parameters, such as crucible nozzle to water level separation (N_W), melt ejection angle (θ), casting temperature, ejection pressure and nozzle orifice diameter (N_D), have similar importance in maintaining the stability of melt jet and solidification rate of the wire and, subsequently, in obtaining good quality wires [5]. The crucible of large orifice diameter (N_D) tends to produce powders due to destabilized melt jet with lower jet velocity impinging into the water. In contrast, the lower limit of N_D is related to higher pressure which is required to overcome the surface tension for the melt ejection. The melt jet is more likely to resist, through surface tension forces, being flattened by the dynamic pressure or drag force of the cooling water. The low melting point alloy is instantaneously solidified on ejecting the melt alloy because of the proximity of cooling water. Thus it is observed empirically that an optimal dwell time before casting is essential to avoid stream disturbance at high temperature melt and nozzle blockage at low temperature melt [5].

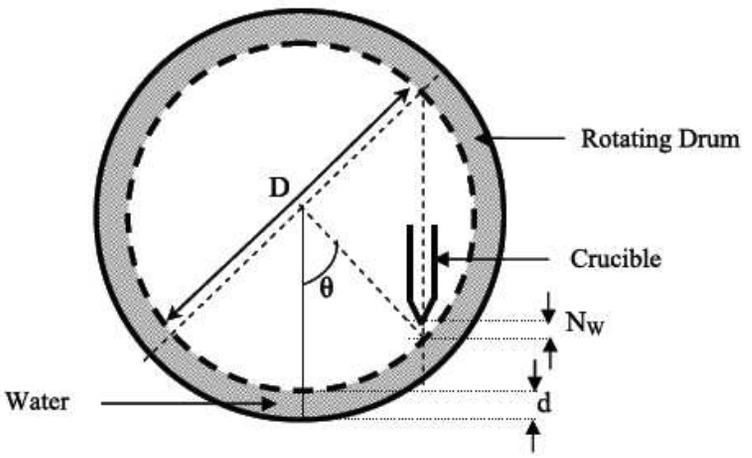

Figure 3. Schematic presentation of in-rotating-water quenching instrument (D: diameter of drum; N_W: separation between nozzle and water surface; d: depth of water level; :ejection angle of the melt) [5].

3. Design of alloy composition

Nanostructured soft magnetic alloys are designed on the basis of refinement of grain size to tailor intrinsic and/or extrinsic magnetic properties. The intrinsic magnetic properties (magnetic flux density, Curie temperature, magnetocrystalline anisotropy, magnetostrictive coefficient) are dependent on alloy chemistry, whereas extrinsic magnetic properties (coercivity, permeability) are influenced by the microstructures. Accordingly, a nanostructured soft magnetic alloy is basically designed with one ferromagnetic and three different non-ferromagnetic elements which are categorized as glass formers, grain growth inhibitors and nucleating agents, as explained schematically in Fig. 4. The stoichiometric variation between these elements lead to a competition between amorphization and crystallinity for obtaining critical ribbon thickness in glassy alloy systems like Fe-Si-B and Co-Si-B (Fig. 5) [6]. It is noteworthy to mention that smaller amount metalloids are required for achieving amorphization and smaller thickness ribbons in Co-based system compared to Fe-based system.

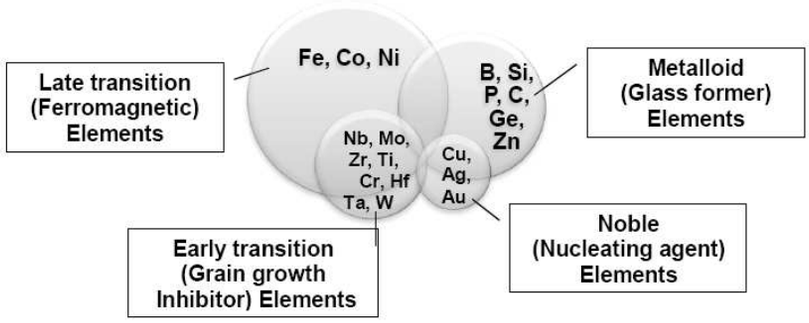

Figure 4. Schematic diagram showing alloy design of soft magnetic alloys (circle diameter representing approximate elemental percentage in alloy).

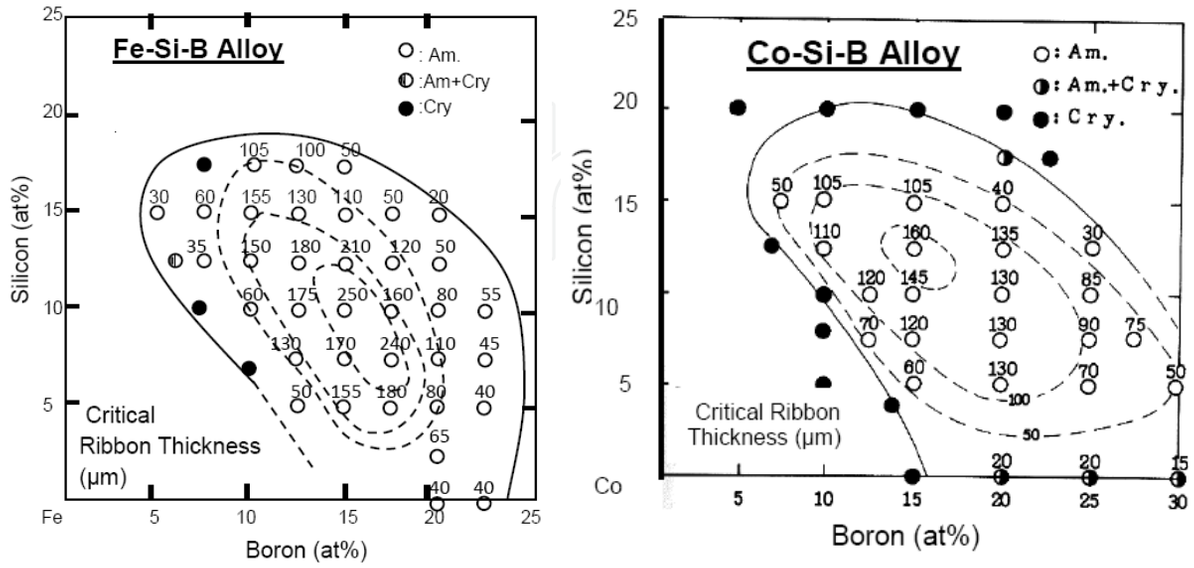

Figure 5. Compositional dependence of amorphization and crystallinity in (a) Fe-Si-B and (b) Co-Si-B systems [6].

Although the elemental composition of nanocrystalline and amorphous alloys may vary within wide ranges, a typical chemical formula may be explained as F_xM_y, where F = ferromagnetic elements (e.g., Fe, Co, Ni), M = non-ferromagnetic elements (e.g., B, Si, P, Nb, Mo, Zr, Cu, etc.), x = 70–90 at% and y = 10–30 at%. According to the compositional ranges of ferromagnetic elements and consequent property developed, nanostructured alloys may be classified as FINEMET (Fe-M-Nb-Cu, where M = B, Si), NANOPERM (Fe-B-Zr-Cu) and HITPERM (Fe-Co-B-Zr-Cu). The composition and magnetic properties of these alloys are explained in Table 1. Therefore, the intrinsic magnetic properties of these alloys are basically the function of ferromagnetic elements, and the extrinsic properties depend on the non-ferromagnetic elements along with the effect of nanocrystallinity. Accordingly, there are three factors to be emphasized during alloy design which are (i) desired magnetic properties, (ii) high thermal stability and (iii) good glass forming ability. Thus, controlled chemistry of nanostructured alloys can cater to different soft magnetic applications pertaining to either ultralow coercivity or high permeability or high Curie temperature or high induction.

Alloy Name	Typical Composition	Saturation Magnetization (T)	Coercivity (A/m)	Permeability	Curie Temp. (T_c), °C
FINEMET	$Fe_{73.5}Si_{13.5}B_9Nb_3Cu_1$	1.24	0.53	10^5	370
NANOPERM	$Fe_{88}Zr_7B_4Cu_1$	1.64	4.5	$3.4X10^4$	770
HITPERM	$Fe_{44}Co_{44}Zr_7B_4Cu_1$	1.6-2.1	-	-	>965

Table 1. Compositions and magnetic properties of three types of amorphous alloys [7]

4. Structure-property correlation

Saturation magnetization and Curie temperature are the intrinsic magnetic properties, depending on alloy chemistry and crystal structure, whereas soft magnetic properties like coercivity and permeability are extrinsic properties, relating to nanocrystallinity of alloys and preferred arrangement of magnetic domains. The soft magnetism of any material is monitored through the coercivity (H_c) and/or permeability (μ), which are inversely related to each other. The excellent soft magnetism is achieved with the tailoring of alloy chemistry and optimizing the microstructure [7].

According to Herzer diagram [8], the relation of soft magnetism with grain size can be divided into two segments, (i) nanocrystalline and (ii) polycrystalline (Fig. 6). For large grain size (D> 0.1–1μm), such as polycrystalline alloys, the coercivity is inversely proportional to D, i.e., H_c 1/D. So, in the segment II, the soft magnetism increases towards right side. In other words, for polycrystalline alloys, the magnetic hardness of fine grained material is larger than that of coarse grained materials. For small grain size (segment-I, D<100nm), such as amorphous and nanostructured alloys, the coercivity rapidly decreases with grain size, and it follows the relation H_c D^6.

http://dx.doi.org/0.5772/60772

In nanostructured materials, the fine (~15 nm diameter) ferromagnetic nanocrystallites are impregnated in the amorphous matrix, and thus magnetic coupling of nanocrystallites exchanges through intergranular amorphous matrix. In other words, the grain sizes in the order of 10–15 nm lowers the magnetocrystalline anisotropy proportionally, resulting in superior soft magnetic properties [8]. Due to higher Curie temperature of nanocrystallites than that of amorphous matrix, the intergranular coupling rapidly decreases while the measuring temperature approaches Curie temperature of amorphous matrix [9]. Since the soft magnetic properties are related to intergranular exchange interaction, Curie temperature of amorphous matrix also plays a dominant role in controlling soft magnetic properties in nanocomposites. If the alloy is designed in such a way that the amorphous matrix has high Curie temperature, the alloy can be used for high temperature applications. Thus a new series of nanostructured alloy named HITPERM was developed which contain equal at% of Fe and Co along with glass former B, nucleating element Cu and the grain growth inhibitor Zr.

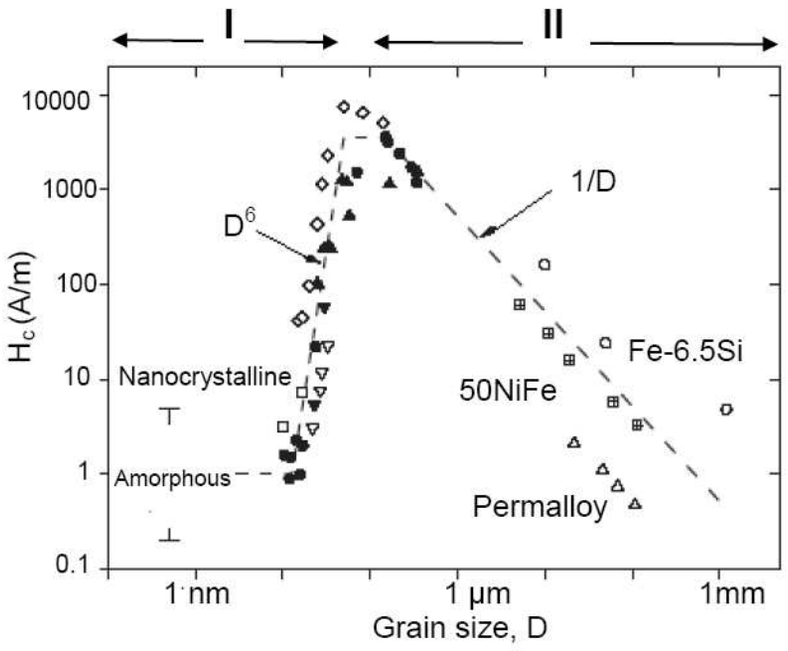

Figure 6. Relationship between coercivity and grain size in soft magnetic alloys as proposed by G.Herzer [8].

In case of HITPERM alloys, the composition variation in amorphous matrix during the nanocrystallization process is a complex function of the enrichment in B, and Nb and increase in the Co/(Fe+Co) ratio. The magnetic properties are thus correlated with nanocrystallites formation in amorphous matrix [10]. Although the Co concentration is homogeneous throughout the amorphous matrix and nanocrystals, Fe is relatively enriched in the amorphous matrix and expels Nb and B to the matrix during crystallization process [11]. The enrichment of matrix with Nb and B stabilizes the residual amorphous phase. Moreover, due to low diffusivity and solubility of Nb in Fe(Co) phases, Nb acts as a diffusion barrier located at the primary nanocrystal/ amorphous matrix interface. The thickness of the diffusion barrier increases with

increasing Nb percentage for fixed B containing alloys. Consequently, it hinders primary nanocrystal grain growth and also restricts Fe enrichment in Fe(Co) phases, resulting into an increase in Fe content in the amorphous matrix and retaining its higher Curie temperature.

5. Different soft magnetic alloys and their properties

Rapid solidification reduces the magnetocrystalline anisotropy, increases the solubility of alloying element and also produces the materials in the form of thin sheet, and hence rolling and forging process can be avoided for many brittle materials. Composition of the materials also plays a vital role in developing soft magnetic materials. A small variation in composition can change intrinsic magnetic property like magnetostriction which in turn alters the magnetoelastic anisotropy of the system and thus, modifies the soft magnetic behaviour of alloys. Alloy compositions have also a strong influence on the crystallization behaviour of rapidly solidified materials. This section will be discussed on the influence of alloy composition for the soft magnetic properties.

5.1. High permeability alloys

The high permeability amorphous alloys may be categorized as FINEMET type alloys with a nominal composition of $Fe_{76.5-x}Si_{13.5}B_9M_xCu_1$ (where M = Nb, Ta, Mo, W, V, Cr and x = 0–3 at%) [12–16]. Many attempts have been made for the modifications of FINEMET alloys, as explained in Table 2. The primary crystallization onset of these alloys approximately 435–500°C, varying with alloy composition. Upon annealing within 50° above primary crystallization temperatures, the α-Fe(Si) nanocrystallites of 10–15 nm grain size are embedded in a residual amorphous matrix, which may be called as nanocomposites. Annealing near or above 600°C leads to the precipitation of boride compounds (Fe_2B or Fe_3B) [17] which is detrimental for soft magnetism of nanostructured materials. The Curie temperature and saturation induction of α-Fe nanocrystallites are about twice than that of amorphous phase for Fe-Si-B-Nb-Cu alloys [18]. However, both magnetic properties decrease with Si percentage in $Fe_{96-z}Si_xB_{z-x}Nb_3Cu_1$. Panda et al. have examined the effect of Si/B ratio on magnetic properties for high temperature annealed alloys $Fe_{73.5}Nb_3Cu_1Si_{22.5-X}B_X$ (X = 5, 9, 10, 11.25, 19) [19]. The magnetic softening has been found maximum at Si/B ratio of 1.5, that is, for the alloy $Fe_{73.5}Nb_3Cu_1Si_{13.5}B_9$, with a coercivity of 1.56A/m and susceptibility of 1.35×10^5 while the alloys is annealed at 527°C. For other Si/B ratio, the magnetic softening is deteriorated before 470°C annealing. In Co added FINEMET alloys, Si has a detrimental effect on saturation magnetization due to the formation of $(Fe,Co)_3Si$ phase than that of (Fe,Co) phase in Si-free alloy, causing less localized moment between Fe and Co atoms in former alloy [20]. On the other hand, Co-based amorphous alloys with small additions of Fe reveal nearly zero λ_s, resulting in good soft magnetic behaviour. Their application is limited due to the fact that their saturation induction is considerably lower compared to that of Fe-based alloys [17].

http://dx.doi.org/0.5772/60772

Alloy Composition	T_{x1} (°C)	T_{x2} (°C)	B_s (T)	Hc (A/m)	μ	Reference
$Fe_{73.5}Si_{13.5}B_9Nb_3Cu_1$	-	-	1.24	0.53	10^5	[21]
$Fe_{73.5}Si_{13.5}B_9Nb_3Cu_1$	497	633	1.23	1.0	35×10^3	[22]
$Fe_{72.5}Si_{13.5}B_9Nb_3Cu_1Al_1$	480	623	1.09	0.74	33×10^3	[22]
$Fe_{73.5}Si_{13.5}B_9Mo_3Cu_1$	487	-	-	-	7×10^3	[23]
$Fe_{73.5}Si_{13.5}B_9V_3Cu_1$	467	577	-	-	750	[23]
$Fe_{36.75}Co_{36.75}Si_{13.5}B_9Mo_3Cu_1$	460	560	-	-	-	[24]
$Fe_{73.5}Si_{17.5}B_5Nb_3Cu_1$	435	615	0.55	1	-	[25]
$Fe_{72.7}V_{1.8}Si_{13.5}B_9Nb_2Cu_1$	-	-	1.21	-	81×10^3	[26]
$Fe_{71.5}Si_{13.5}B_9Nb_3Cu_1Al_2$	-	-	1.3	0.32	-	[27]
$Fe_{62.8}Co_{10}Si_{10}B_{13.5}Nb_3Cu_{0.7}$	572	662	1.35	3	-	[28]

Table 2. Thermal and magnetic properties of some FINEMET alloys

(T_{x1} = Primary crystallization temperature onset, T_{x2} = secondary crystallization temperature onset, B_s = saturation induction, H_c = coercivity and μ = permeability)

5.2. High induction alloys

In high permeability alloys, the distribution of fine nanocrystallites in amorphous precursor is a key factor for the improvement of soft magnetism. This is attributed to the presence of high (>20 at%) metalloids by replacing ferromagnetic elements, like Fe, Co, Ni, etc. As a result, alloys like FINEMET have superior soft magnetic properties, but the saturation induction of these alloys is lower than that of Si steel. To fill up this dearth, many high (>1.24T) induction alloys have been developed in recent years (Table 3).

Alloy Composition	B_s (T)	H_c (A/m)	μ	Reference
$Fe_{83.16}P_{4.95}C_{3.96}B_{3.96}Si_{2.97}Cu_1$	1.74	4.9	22.9×10^3	[29]
$Fe_{82.65}B_{14}Si_2Cu_{1.35}$	1.85	10	-	[30]
$Fe_{83.7}Nb_{6.6}B_{8.6}P_1Cu_{0.1}$	1.5	5	48×10^3	[31]
$Fe_{81.7}P_2B_7Si_9Cu_{0.3}$	1.56	7	-	[32]
$Fe_{85}P_4B_8Si_2Cu_1$	1.85	6.1	27×10^3	[33]
$Fe_{91}Zr_7B_2$	1.7	7.2	14×10^3	[34]
$Fe_{89}Zr_7B_3Cu_1$	1.64	4.5	34×10^3	[35]
$Fe_{86}Zr_7B_3Si_4$	1.54	-	10^4	[36]
$Fe_{53.3}Co_{28.7}Si_{2.8}B_{11.2}Nb_3Cu_1$	1.54	-	-	[37]
$Fe_{55.25}Co_{29.75}Si_{2.8}B_{11.2}Cu_1$	1.73	-	-	[37]
$Fe_{54.6}Co_{29.4}Si_{2.8}B_7P_{4.2}Nb_1Cu_1$	1.62	-	-	[38]

Table 3. Saturation induction (B_s), coercivity (H_c) and permeability (μ) of some amorphous alloys

The design of high induction alloys may be based on Slater-Pauling curve [42], which explains the high magnetic induction achievable in Fe-Co alloys compared to either Fe- or Co- based alloys (Fig. 7). The Curie temperature is also high in these alloys than Fe-rich alloys. The crystalline alloys of $Fe_{65-70}Co_{35-30}$ exhibit maximum saturation induction and Curie temperature of 2.4T and 1000°C, respectively [39]. These values are deteriorated in amorphous or nano-crystalline alloys due to the additions of metalloids and other elements. However, many Fe-based alloys have been explored with a saturation of 1.85T rather than Fe-Co based alloys (Table 3). Although the Curie temperature of former alloys may be lower than later alloys. The minimum magnetocrystalline anisotropy is investigated at concentration of x = 0.5 for $Fe_{1-x}Co_x$ system [39]. The magnetostriction coefficient (λ_s) is also significant in equiatomic composition of this alloy system. Since Fe is positively magnetostrictive, addition of negatively magnetostrictive Co to Fe reduces the overall magnetostriction λ_s of $Fe_{80-x}Co_xB_{20}$ system [39]. Similarly addition of Co to Fe raises the saturation induction as depicted in Slater Pauling curve with the maximum saturation magnetization value reported for $Fe_{70}Co_{10}B_{20}$ alloy [41].

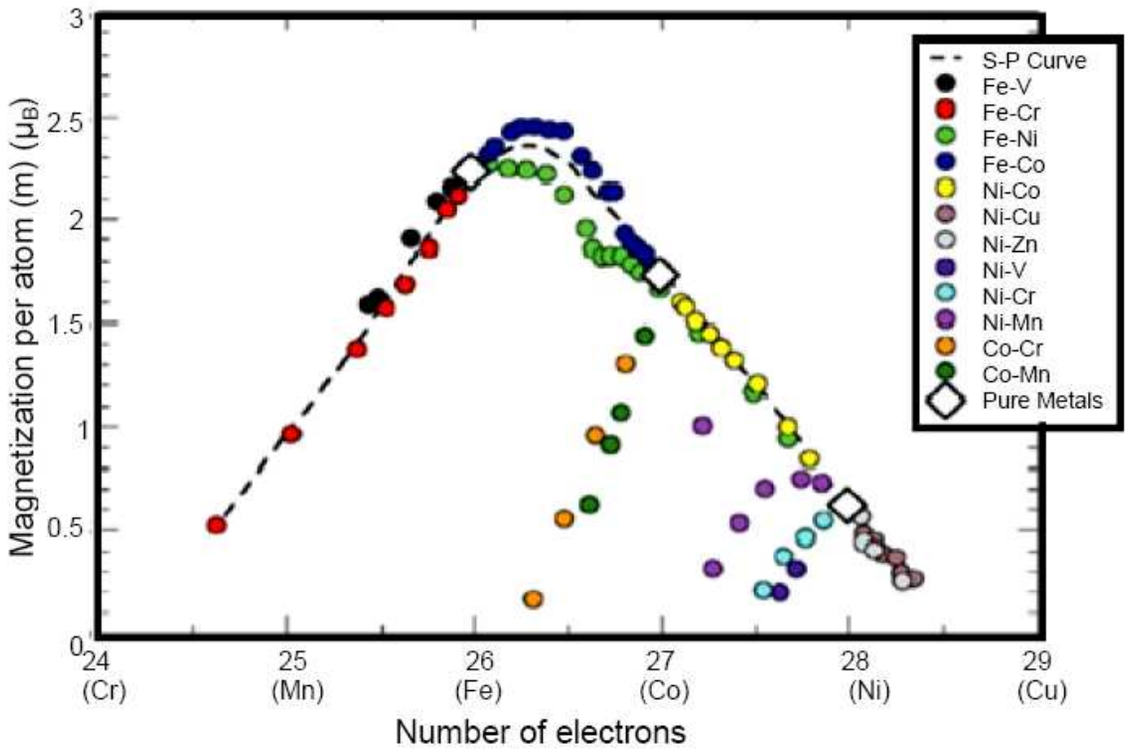

Figure 7. Slater-Pauling curve of late transition elements [42].

5.3. Fe-6.5 wt% Si steel

The development of high silicon (Si) steels bears technological as well as commercial importance not only due to their superior soft magnetic properties but also due to low cost. The 3.5

wt% Si steel has a major application in distribution transformers owing to their excellent soft magnetic properties and low core losses [43]. This material is being produced in the form of cold rolled grain oriented (CRGO) or non-grain oriented (CRNO) Si steel. Increasing Si content beyond 3.5% in iron enhances the electrical resistivity of the alloy, resulting in low eddy current component. Si also decreases the magnetostriction constant which becomes minimum at 6.5 wt%, leading to improved soft magnetic properties and low core losses [43]. However, the workability of alloy deteriorates with enhancement in Si content due to the formation of some ordered phases B2 and DO_3 (see Fig. 8), coarse grains and impurities on grain boundary, etc. [44, 45]. Therefore, the fabrication of strips with high ~6.5 wt% silicon through conventional rolling process is difficult owing to inherent brittleness of the material [47]. The brittleness is due to the formation of ordered phases, coarser grains and impurities on grain boundary, etc. A breakthrough in the improvement of ductility by suppression of ordered phases may be was achieved while processing the alloy through several rapid solidification techniques like chemical vapour deposition (CVD), gas atomization, splat quenching and melt spinning [48–50]. The products of these processes are subjected to various annealing treatments to control the grain sizes and ordered phases for achieving superior soft magnetic properties [51]. Amongst these methods, the development of 6.5 wt% Si steel ribbons by melt spinning technique has drawn an intense research interest due to its potential for production in bulk quantities demand as a high-efficiency material for magnetic components [52, 53].

In the Fe-Si alloys, mainly one disordered structure A2 and two types of ordered phases, viz., B2 (FeSi type) and DO_3 (Fe_3Si type) structures are observed within 5.5 to 10 wt% Si contents [54]. The ordered phases B2 and DO_3 are superstructures of A2. They form from A2 phase by unlike-atom pairing of first and second nearest neighbor place in BCC lattice, respectively [53]. It is observed that melt spun ribbons comprise mainly A2 disordered phases owing to the suppression of ordered phases [52]. Subsequent heat treatment can bring about second order transformation of A2 to B2 phase, as shown in the Fe-Si phase diagram (Fig. 8). However, B2 to DO_3 transformation which is of first order can take place simultaneously, leading to the co-existence of both these phases [55]. The grain size becomes finer and the ductility is also improved in the rapidly solidified ribbons. Therefore, the rapid solidification route emerges as a potential technique for the fabrication of Fe-6.5 wt % Si alloys [50, 55]. During the course of annealing treatment, the ordered phases B2 and DO_3 form and affect the magnetic properties.

It is reported that the as-cast 6.5 wt% Si steel ribbon shows low permeability (μ_m ~ 1.13×10^{-3}) and high coercivity (H_c ~150A/m) owing to large internal stress and grain refinement caused by rapid solidification (Fig. 9) [56]. With progress of annealing, the maximum permeability continuously increases with annealing temperature and gets saturate after 800ºC. Conversely, the coercivity decreases linearly with the annealing temperature and gets the lowest value after annealing at 850ºC. Therefore, the soft magnetic properties are quite improved by controlling the distribution and size of ordered phases [58]. In this regard, the post annealing treatment has an influential effect on the morphologies of ordered phases [59].

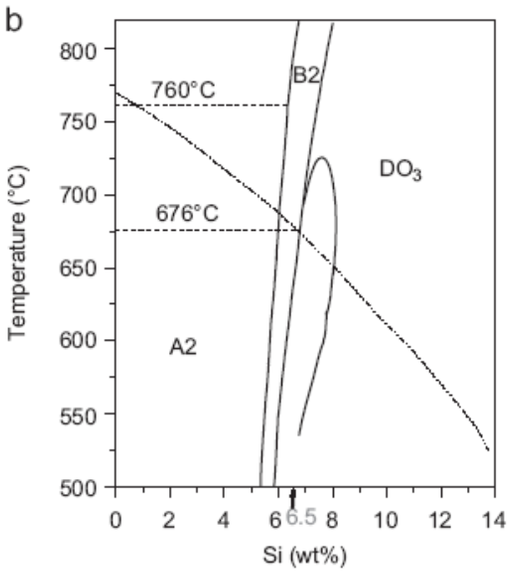

Figure 8. Fe-Si Phase diagram [54]

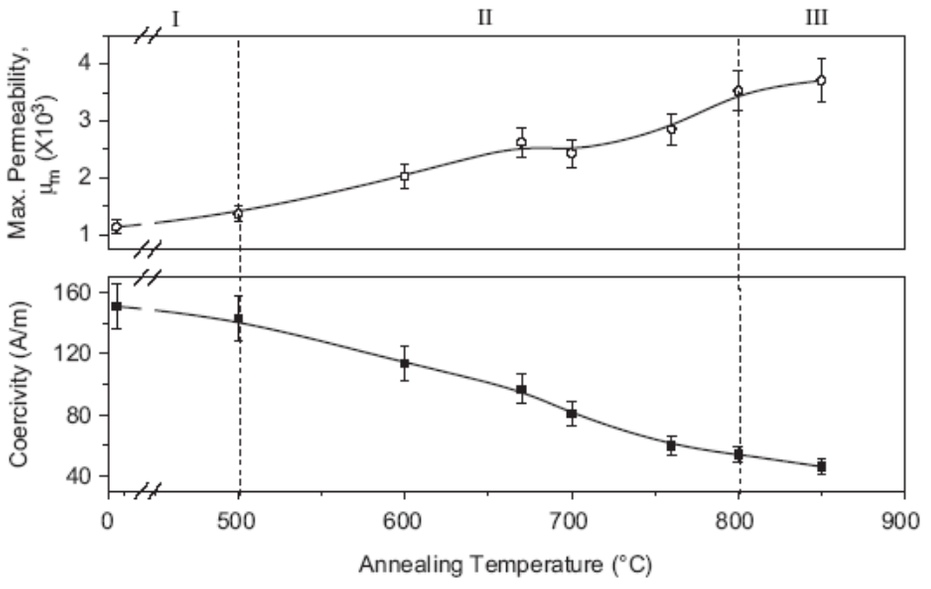

Figure 9. Variation of maximum permeability and coercivity as a function of annealing temperature [57].

5.4. Alloys with giant magnetoimpedance properties

An interesting phenomenon called giant magneto-impedance (GMI) where large magnetic field dependence of electrical impedance (Z) is observed in ferromagnetic wire prepared by in-rotating water quenching technique (discussed in section-2.2). Unlike the well-known phenomena of GMR where large change in material resistance takes place upon application of magnetic field, complex impedance suffers drastic changes as a function of external

http://dx.doi.org/0.5772/60772

magnetic field in GMI materials within the frequency range of 100 kHz to few MHz. GMI behaviour is also observed in ribbon-shaped materials, but the value in wire-shaped material exhibits much higher value. The influence of external magnetic field on the skin depth is the major cause for large change in magnetoimpedance of rapidly solidified wire. The skin depth of the materials is expressed as

$$\delta = \frac{c}{\sqrt{4\pi^2 f\sigma\mu}},$$

where μ is the material permeability, c is the speed of light, σ is the electrical conductivity and is frequency of the ac current used for measuring GMI voltage.

The circular permeability is a function of external magnetic field, temperature and also stress. Thus the impedance in rapidly solidified wire changes not only with the external magnetic field but also with temperature and stress. Hence, the GMI materials have potential application as field, temperature and stress sensors. Anisotropy in rapidly solidified materials is predominantly magnetoelastic in origin. Thus the value of saturation magnetostriction constant plays major roll in controlling the circular permeability and hence the skin depth. The materials with low magnetostriction constant exhibit higher response in impedance under the influence of applied magnetic field. Thus the materials should be designed in such a way that their saturation magnetostriction constant should be very low. Usually, Co-based amorphous alloys have negative magnetostriction (λ_s ~ -3×10^{-6}), whereas Fe-based alloys have positive magnetostriction value (λ_s ~ 25×10^{-6}). An alloy with the combination of Fe and Co will provide low saturation magnetostriction and expected to be the better GMI materials.

The GMI materials are characterized by GMI ratio (Z/Z) which is the normalized value of magnetoimpedance with respect to high magnetic field and expressed as:

$$\frac{\Delta Z}{Z}(\%) = \frac{Z(H) - Z(H_{MAX})}{Z(H_{MAX})} \times 100\%$$

where Z(H) is the impedance of the material with the applied magnetic field H and Z(H_{max}) is magnetic field saturating the impedance [60].

Moreover, the Fe-, Co- and FeCo-based alloys reveal different GMI properties depending on the core–shell domain structure of the wires [60]. The Fe-based microwires (e.g., Fe-Si-B) possess cylindrical domain with longitudinal magnetization and radially closure domains. Such domain patterns attribute to a large Barkhausen effect (LBE) in the wire [61]. The LBE causes a square loop in positively magnetostrictive FeSiB systems, leading to a perspective use in switching devices [62, 63]. On the other hand, the Co-based wires (e.g., Co-Si-B) have bamboo shaped circular domains in the wire outer surface, resulting in large Barkhausen effect (LBE) and axial pattern in inner core. Such differences in domain pattern in Fe-based and Co-based alloys arise due to their positive and negative magnetostriction, respectively. Garcia et

al. has reported a large GMI ratio of 1200% at 14.2 MHz for the zero magnetostrictive amorphous microwire $Co_{68}Fe_{4.35}Si_{12.5}B_{15}$ [64]. However, other researchers have reported a lower (600%) GMI ratio for the same composition [65, 66]. Recently, the Cr addition has revealed the improvement of GMI effect as well as field sensitivity in amorphous wires with nominal composition of $(Co_{0.5}Fe_{0.5})_{78-x}Cr_xSi_8B_{14}$ (X = 0 to 12 at%), where saturation magnetostriction of the materials changes with the Cr [67]. Fig. 10 shows the change of GMI ratio with the saturation magnetostriction at driving current (I_{ac}) = 10mA and the driving frequency 400 kHz. The variation of maximum GMI ratio (GMI_{max}) with Cr for as-quenched and annealed wires is shown in Fig. 11.

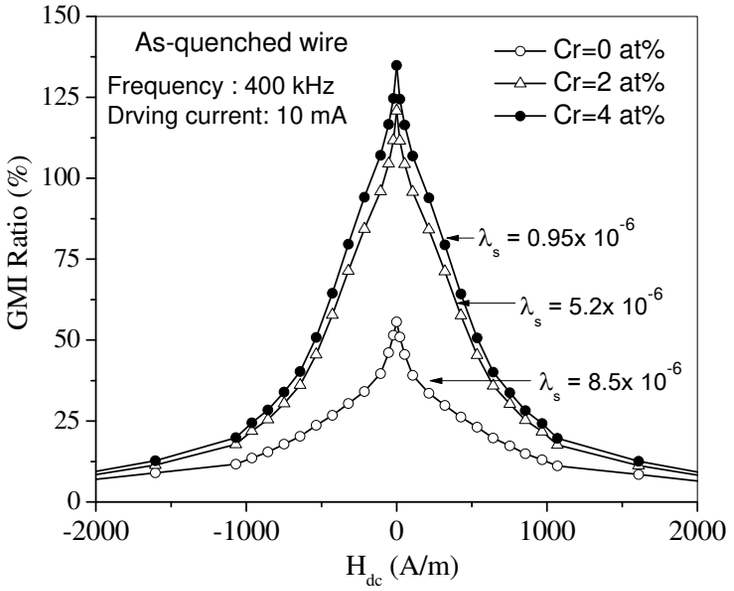

Figure 10. GMI plots of Cr-0, Cr-4, Cr-7 for as-quenched wires showing variation of GMI ratio with the saturation magnetostriction constant of the materials $(Co_{0.5}Fe_{0.5})_{78-x}Cr_xSi_8B_{14}$ (X = 0, 4, 7 at%)

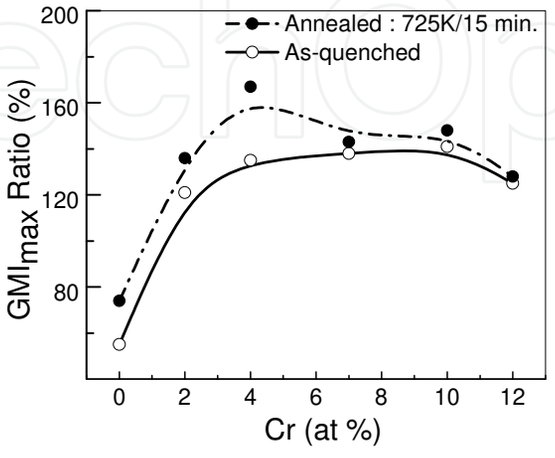

Figure 11. Effect of annealing on GMI_{max} with Cr content in $(Co_{0.5}Fe_{0.5})_{78\_x}Cr_xSi_8B_{14}$ (x = 0 to 12 at%) wires

http://dx.doi.org/0.5772/60772

6. Applications

The uniqueness of rapidly solidified amorphous and nanocrystalline materials is that the structural correlation (grain size) is much smaller than the ferromagnetic correlation length (domain wall with) [17]. It causes the lowering of magnetocrystalline anisotropy, and there is a tendency of vanishing magnetostriction for certain alloy compositions. As a consequence, nanocrystalline alloys achieve superior soft magnetic properties. Moreover, the improved other magnetic properties, such as higher saturation induction, Curie temperature, thermal stability of some FeCo-based amorphous and nanocrystalline alloys (HITPERM) envisage the reduction in size and weight of magnetic components, and therefore, it can be affective for the versatile applications of these alloys.

Accordingly, the nanocrystalline soft magnetic alloys may be applicable in the following field such as

i. Core material for power transformer and magnetic choke coil

ii. Inductive components for switched mode power supplies

iii. Magnetic sensors

The performance of magnetic choke coil made using FINEMET alloys is improved than that of Mn-Zn ferrite based choke coil [12–13]. The NANOPERM choke coil is also effective to prevent signal distortion in reactor elements of the phase modifying equipment [68]. Owing to high saturation induction, good thermal stability and low core loss, the NANOPERM alloys can also be applicable as a core material for high frequency power transformer [35]. Some FeCo-based amorphous alloys (HITPERM) have a demand as core materials and winding wires for audio and radio frequency transformers in space power system [7]. These materials may also be applicable as a rotor assembly in More-Electric Aircraft Integrated Power Unit (MEA-IPU).

Beside the applications in the field of transformer, rapidly solidified materials are widely used as core materials for sensors and transducers. A wide range of magnetic sensors, such as induction sensors, fluxgate sensors (FGS), Hall Effect sensors, giant magnetoresistive sensors and superconducting quantum interference device (SQUID) gradiometers are available. A magnetic sensor directly converts the magnetic field into some measurable parameters and the field sensitivity of the sensor plays a key role in determining its operating regime and potential applications. High permeability of amorphous and nanostructured materials are rapidly replacing their crystalline counterpart to achieve better performance of the sensing device.

The GMI effect has attracted considerable scientific and technological interest especially because of its applicability in magnetic field sensing and as an additional tool to investigate soft magnetic properties of other materials, for example, ferritic steel. Magnetic sensors based upon the GMI effect offer several advantages over conventional magnetic sensors. Amorphous metallic materials cast in the form of wire having diameter of the order of 100 μm are generally used as the core of this type of magnetic sensors. These materials have their superior mechanical, electrical and magnetic properties which originate from the absence of long range order. The formation of amorphous state depends on the alloy composition as well as on the

processing condition. The microwires with large and positive magnetostriction, exhibit bistable behaviour with magnetization reversal through a giant Barkhausen jump originating in the propagation of a single-domain wall. On the other hand, microwires with very low or vanishing magnetostriction show excellent GMI effect. Both the types show natural ferromagnetic resonance (NFMR) at microwave frequencies.

The GMI materials can be used as the magnetic field and current sensors because GMI changes as a function of external dc magnetic field or applied dc/ac currents, respectively. The sensing elements of GMI sensors are in the form of amorphous wires [69], thin films [70] or ribbons [71]. The Aichi Steel Corporation of Japan has designed and developed a variety of GMI sensors using amorphous wires for a wide range of technological applications [72]. Since GMI effect is dependent on the applied stress, it is possible to design and develop stress and magnetoelastic sensors using Co-based amorphous ribbons and wires, respectively [73, 74]. Recently, GMI sensors have been projected for structural health monitoring of industrial components [75]. Additionally, many GMI sensors have been proposed for car traffic monitoring, antitheft system, electronic compass, non-destructive crack detection, detection of ferromagnetic dust inside human body, tyre pressure monitoring system, etc. [60].

GMI phenomena attracted a great attention for the sensor applications owing to the large sensitivity of the electrical impedance to the DC magnetic field of soft magnetic conductor [76]. The ultra-high sensitivity of GMI to external dc magnetic field (down to 10^{-4} A/m) can be used for magnetic field sensors and other sensors based on the change of a local magnetic field.

All these novel properties make amorphous magnetic microwires very attractive for exceptional technological applications, and also provide opportunities for fundamental micromagnetic studies mainly due to their unique magnetic domain structure. The sensitivity of GMI sensors is found to be high and have improved characteristics among the micromagnetic sensor families (Table 4) [77, 78].

Sensor element	**Hall**	**Giant magnetoresistive sensors**	**Flux gate sensor (FGS)**	**Giant magnetoimpedance (GMI) sensors**
Materials	In-Sb, Ga-As	Multilayer thin film	Fe-Ni	Amorphous wire/glass coated
Parameter	Hall voltage	Magnetoresistance	Magnetic flux	Magnetoimpedance
Field detection (A/m)	$0.1–2\times10^{5}$	10–20k	$10^{-4}–10^{-2}$	$10^{-4}–10^{-2}$
Frequency	0–5 kHz	0–10MHz	0 –10kHz	0.1–10MHz
Head size (mm)	0.1	0.01–0.1	3–20	0.1–3
Resolution (A/m)	10^{-2}	10^{-2}	10^{-4}	10^{-4}
Sensitive axis	Perpendicular	Parallel	Parallel	Parallel
Power consumption	1W	10mW	1W	10mW

Table 4. Micromagnetic sensor families and properties of sensor elements

http://dx.doi.org/0.5772/60772

Such type of magnetic field sensor can be extended for non-invasive way of monitoring the structural health of steel components which are in-service and intended to use for an extended period during which various damages can be developed such as residual stress, fatigue, creep or the formation of magnetic phase in non-magnetic steel in non-destructive way.

7. Conclusion

Rapidly solidified soft magnetic materials have been placed in special class of functional materials due to their excellent soft magnetic properties. They can be used as a transformer core or sensing element depending on composition. Due to low core loss and subsequently less heating effect, amorphous metal core transformers are slowly replacing the conventional Si steel–based distribution transformer. However, these materials are not suitable for power transformer as the saturation induction is lower than the crystalline counterpart due to the presence of non-magnetic metalloid. Extensive research is now going on to enhance the saturation induction by increasing the ferromagnetic components. The bulk production of rapidly solidified materials for transformer are mainly carried out by Hitachi Metals, Japan; Metglas, USA; Advanced Technology and Materials Co. Ltd (AT&M), China; POSCO, Korea which are the major players for large scale production of amorphous materials for transformer core where about 90 mm wide ribbons are required. Nanostructured materials are slowly replacing the core for small scale transformer like Switched Mode Power Supply (SMPS), circuit breaker and also for various types of sensor development. Nanostructured magnetostrictive wires are excellent element for pulse generating sensor application due to their large Barkhausen effect. Nearly zero magnetostrictive wires are excellent materials for GMI-based sensor element used for magnetic field determination.

Author details

Rajat K. Roy*, Ashis K. Panda and Amitava Mitra

*Address all correspondence to: rajat@nmlind.org, rajatroy.k@gmail.com

MST Division, CSIR-National Metallurgical Laboratory, Jamshedpur, India

References

[1] H. H. Liebermann, *Ribbon- substrate adhesion dynamics in chill block melt spinning processes*, Metall. Trans. B, 15 (1984) 155–161.

[2] Huang et al., *Rapidly solidified amorphous and crystalline alloys*, Ed. by B.H. Kear, B.C.Giessen, M. Cohen, Material Research Society, 1981, pp. 211–216

[3] B. Heyder, G.Frommeyer, *Direct casting of continuous fibres and wires by in-rotating-liquid spinning*, Mater. Sci. Eng., A, 133 (1991) 667–670.

[4] A. O. Olofinjana, J. H. Kern, H. A. Davies, *Effects of process variables on the multi-strand casting of high strength sub-millimeter metallic glass wire* J. Mater. Process Technol., 155–156 (2004) 1344–1349.

[5] P. Sarkar, R. K. Roy, A. K. Panda, A. Mitra, *Optimization of process parameters for developing FeCoSiB amorphous microwires through in-rotating-water quenching technique*, App. Phys. A: Mater. Sci. Process, 111 (2013) 575–580.

[6] L. Schultz, *Formation of amorphous metals by mechanical alloying*, Ed. by M. Von Allmen, Proc. MRS Europe Meet. on Amorphous Metals and Non-Equlibrium Processing, 1984, p. 135.

[7] M. E. McHenry, M. A. Willard, D. E. Laughlin, *Amorphous and nanocrystalline materials for applications as soft magnets,* Prog. Mater Sci., 44(1999) 291–433.

[8] G. Herzer, *Nanocrystalline soft magnetic alloys*, in Handbook of magnetic materials, Ed. by K. H. J. Buschow, vol. 10. Amsterdam: Elsevier Science BV; 1997.

[9] A. Mitra, A. K. Panda, S. R. Singh, V. Rao, P. Ramachandrarao, *Magnetic and structural behaviours of nanocrystalline Fe70.8Nb3.7Cu1Al2.7Mn0.7Si13.5B7.6 alloy*. Philos. Mag., 83 (2003) 1495–1509

[10] M. E. McHenry, F. Johnson, H. Okumura, T. Ohkubo, A. Hsiao, V. R. V. Ramanan, D. E. Laughlin (invited), *The kinetics of nanocrystallization and microstructural observations in FINEMET, NANOPERM and HITPERM nanocomposite magnetic materials*, Scripta Mater., 48(2003) 881.

[11] Y. Zhang, J. S. Blázquez, A. Conde, P. J. Warren, A. Cerezo, *Partitioning of Co during crystallisation of Fe–Co–Nb–B(–Cu) amorphous alloys,* Mater Sci. Eng., A, 353 (2003) 158.

[12] Y. Yoshizawa, S. Oguma, K. Yamauchi, *New Fe-based soft magnetic alloys composed of ultrafine grain structure,* J. Appl. Phys., 64(1988) 6044.

[13] Y. Yoshizawa, K. Yamauchi, T. Yamane, H. Sugihara, *Common mode choke cores using the new Fe-based alloys composed of ultrafine grain structure,* J. Appl. Phys., 64 (1988) 6047.

[14] Y. Yoshizawa, K. Yamauchi, J. Jpn. Inst. Met., 53(1989) 241.

[15] Y. Yoshizawa, K. Yamauchi, Mater Trans., JIM, 31(1990) 307.

[16] Y. Yoshizawa, K. Yamauchi, *Magnetic properties of Fe-Cu-M-Si-B (M = Cr, V, Mo, Nb, Ta, W) alloys,* Mater Sci. Eng., A,133(1991) 176.

[17] G. Herzer, *Modern soft magnets: amorphous and nanocrystalline materials,* Acta Mater., 61 (2013) 718–734.

[18] G. Herzer, IEEE Trans Magn., MAG-25 (1989) 3327.

[19] A. K. Panda, B. Ravikumar, S. Basu, A. Mitra, *Crystallization and soft magnetic properties of rapidly solidified Fe $_{73.5}$ Nb3Cu1Si $_{22.5-X}$ B $_{X}$ (X=5, 9, 10, 11.25, 19) alloys*, J. Magn. Magn. Mater., 260 (2003) 70–77

[20] M. A. Willard, M. Daniil, K. E. Kniping, *Nanocrystalline soft magnetic materials at high temperatures: A perspective,* Scripta Mater., 67 (2012) 554.

[21] Y. Zhang, K. Hono, A. Inoue, T. Sakurai, *Partitioning of Si in a Fe87Zr7Si4B2 nanocrystalline soft magnetic alloy,* Appl. Phys. Lett., 69(1996) 2128.

[22] S. H. Kim, W. K. Pi, T. H. Noh, H. J. Kim, I. K. Kang, *Effects of Al on the magnetic properties of nanocrystalline Fe73.5Cu1Nb3Si13.5B9 alloys,* J. Appl. Phys., 73(1993) 6591.

[23] X. Z.Zhou, A. H. Morrish, D. G. Naugle, R. Pan, *Mössbauer study of amorphous and nanocrystalline Fe73.5Cu1Nb3Si13.5B9,* J. Appl. Phys., 73(1993) 6597.

[24] J. Wang, Z. Wang, Y. Jia, R. Shi, Z. Wen, *High temperature soft magnetic properties of (FexCo1−x)73.5Cu1Mo3Si13.5B9 (x=0.5,1) alloys*, J. Magn. Magn. Mater., 328 (2013) 62–65

[25] T. Kulik, A. Hernando, M. Vazquez, *Correlation between structure and the magnetic properties of amorphous and nanocrystalline Fe73.5Cu1Nb3Si22.5−x Bx alloys*, J. Magn. Magn. Mater., 133(1994) 310.

[26] A. R. Yavari, D. Negri, Nanostruct. Mater., 8(1997) 969.

[27] L. K. Varga, A. Lovas, L. Pogany, L. F. Kiss, J. Balogh, T. Kemeny, *The role of nucleating element additives in the crystallization and soft magnetic properties of Fe-Zr-B based amorphous alloys*, Mater Sci. Eng., A226–228(1997) 740.

[28] B. Shen, A. Inoue, J. Mater. Res., 19(2004) 2549–2552.

[29] M. Zhang, A. Wang, W. Yang, B. Shen, *Effect of Fe to P concentration ratio on structures, crystallization behavior, and magnetic properties in (Fe0.79+xP0.1-xC0.04B0.04Si0.03)99Cu1 alloys*, J. Appl. Phys., 113, 17A337 (2013)

[30] M. Ohta, Y. Yoshizawa, Appl. Phys. Lett., *Magnetic properties of nanocrystalline Fe 82.65 Cu 1.35 Si x B 16−x alloys(x=0–7), 91, (2007) 062517*.

[31] A. Makino, M. Bingo, T. Bitoh, K. Yubuta, *Improvement of soft magnetic properties by simultaneous addition of P and Cu for nanocrystalline FeNbB alloys,* A. Inoue, J. Appl. Phys., 101, 09N117(2007)

[32] A. Makino, H. Men, K. Yubuta, T. Kubota, *Soft magnetic FeSiBPCu hetero-amorphous alloys with high Fe content,* J. Appl. Phys., 105, 013922(2009)

[33] T. Kubota, A. Makino, A. Inoue, *Low core loss of Fe $_{85}$ Si $_{2}$ B $_{8}$ P $_{4}$ Cu $_{1}$ nanocrystalline alloys with high B $_{s}$ and B $_{800}$,* J. Alloys Compd., 509 (2011) S416-S419.

[34] K. Y. Kim, T. H. Noh, I. K. Kang, T. Kang, *Microstructural change upon annealing Fe-Zr-B alloys with different boron contents,* Mater Sci. Eng. A,179/180 (1994) 552.

[35] A. Makino, A. Inoue, T. Masumoto, Mater. Trans., JIM, 36(1995) 924.

[36] A. Inoue, Y. Miyauchi, A. Makino, T. Masumoto, Mater. Trans., JIM, 37(1996) 78.

[37] R. K. Roy, S. J. Kernion, S. Shen, M. E. McHenry, *Crystallization behavior and high temperature magnetic phase transitions of Nb-substituted FeCoSiBCu nanocomposites,* App. Phys. Lett., 99 (2011) 192506.

[38] R. K. Roy, S. Shen, S. J. Kernion, M. E. McHenry, *Effect of P addition on nanocrystallization and high temperature magnetic properties of low B and Nb containing FeCo nanocomposites*, J. App. Phys., 111, (2012) 07A301.

[39] F. Pfeifer, C. J. Radelo€, *Soft magnetic Ni-Fe and Co-Fe alloys - some physical and metallurgical aspects.*, J. Magn. Magn. Mater., 19(1980) 190.

[40] R. Boll, H. R. Hilzinger, H. Warlimont, The magnetic, chemical and structural properties of glassy metallic alloys, Ed. by R. Hasegawa, Boca Raton, FL: CRC Press; 1983.

[41] R. C. O'Handley, R. Hasegawa, R. Ray, C.P. Chou., *Ferromagnetic properties of some new metallic glasses,* Appl. Phys. Lett., 1976; 29(6): 330–332.

[42] J. C. Slater, *The Ferromagnetism of Nickel. II. Temperature Effects*, Phys. Rev. 49 (1936) 931.

[43] L. Pauling, *The Nature of the Interatomic Forces in Metals*, Phys. Rev. 54 (1938) 899.

[44] K. Narita, M. Enokizono, *Effect of nickel and manganese addition on ductility and magnetic properties of 6.5% silicon-iron alloy,* IEEE Trans Magn., MAG-14 (1978) 258

[45] D. Bouchara, M. Fagot, J. Degauque, J. Bras, *Ordering influence on magnetic properties of rapidly quenched Fe-6.5 wt% Si*, J. Magn. Magn. Mater., 83 (1990) 377.

[46] B. Viala, J. Degauque, M. Barico, E. Ferrara, F. Fiorillo, *Study of the brittle behaviour of annealed Fe-6.5 wt%Si ribbons produced by planar flow casting,* Mater. Sci. Eng., A, 212 (1996) 62.

[47] H. Haiji, K. Okada, T. Hiratani, M. Abe, M. Ninomiya, *Magnetic properties and workability of 6.5% Si steel sheet,* J. Magn. Magn. Mater., 160 (1996) 109.

[48] P. R. Swann, L. Grånäs, B. Lehtinen, Met. Sci., 9 (1975) 90–96.

[49] K. Narita, Y. Enokizono, N. Teshima, Y. Mori, *Magnetic properties of 6.5% silicon-iron ribbon produced by splat-cooling technique,* J. Magn. Magn. Mater., 19 (1980) 143.

[50] Y. Takada, J. Appl. Phys., 64 (1988) 5367.

[51] Y. Sato, T. Sato, Y. Okazaki, *Production and properties of melt-spun Fe-6.5wt.%Si ribbons*, Mater. Sci. Eng., 99 (1988) 73.

[52] X. F. Bi, Y. Tanaka, K. Sato, *Effect of microstructure on the magnetic properties of 6.5% Si-Fe alloy,* J. Magn. Magn. Mater., 112 (1992) 189.

[53] K. Narita K, N. Teshima, Y. Yamashiro, Y.J. Shin, Y. Yoshida, *Magnetic properties of rapidly quenched silicon-iron ribbons,* J. Magn. Magn. Mater., 41 (1984) 86.

[54] M. Enokizono, N. Teshima, K. Narita, IEEE Trans Magn., MAG-18 (1982) 1007.

[55] O. Kubaschewski, Iron Binary Phase Diagram, Springer, Berlin, 1982, p.136.

[56] H. R. Hilzinger, *Recent advances in rapidly solidified soft magnetic materials*, J. of Magn. Magn. Mater., 83 (1990) 370.

[57] S. K. Das, C. F. Chang, L. Richard, *Heat treatment of rapidly quenched Fe-6.5 wt% Si ribbon*, US Patent No 4865657 (1989).

[58] R. K. Roy, A. K. Panda, M. Ghosh, A. Mitra, R. N. Ghosh, *Effect of annealing treatment on soft magnetic properties of Fe–6.5 wt% Si wide ribbons*, J. Magn. Magn. Mater., 321 (2009) 2865.

[59] F. E. Luborsky, J. L. Walter, *Stability of amorphous metallic alloys*, J. Appl. Phys. 47 (1976) 3648–3650.

[60] J. E. Wittig, G. Frommeyer, *Deformation and Fracture Behavior of Rapidly Solidified and Annealed Iron-Silicon Alloys*, Metall. Trans. A, 39A, (2008) 252.

[61] M. H. Phan, H. X. Peng, *Giant magnetoimpedance materials: Fundamentals and applications*, Prog. Mater. Sci., 53 (2008) 323-420.

[62] P. Ripka, Magnetic Sensors and Magnetometers, Artech House Publishers, Boston, London, 2001.

[63] H. Chiriac, T.A. Ovari, *Amorphous glass-covered magnetic wires: Preparation, properties, applications,* Prog. Mater Sci., 40 (1996) 333.

[64] M. Vazquez, A. Hernando, J. App. Phys., 299 (1996) 39.

[65] D. Garcia, V. Raposo, O. Montero, I. J. Inguez, *Influence of magnetostriction constant on magnetoimpedance–frequency dependence*, Sens. Actuators, A, 129 (2006) 227–230.

[66] M. Vazquez, M. Knobel, M. L. Sanchez, R. Valenzuela, *Giant magnetoimpedance effect in soft magnetic wires for sensor applications*, Sens. Actuators, A, 59 (1997) 20–29.

[67] M. Vazquez, *Giant magneto-impedance in soft magnetic "Wires"*, J. Magn. Magn. Mater., 226-230 (2001) 693.

[68] P.Sarkar, A. Basu Mallick, R. K. Roy, A. K. Panda, *Structural and Giant Magneto-impedance properties of Cr-incorporated Co–Fe–Si–B amorphous microwires,* A. Mitra, J. Magn. Magn. Mater., 324 (2012) 1551–1556

[69] I. Navarro, A. Hernando, *Magnetic and structural properties of nanocrystalline Fe77B19Cu1Nb3 alloy,* J. Magn. Magn. Mater., 133(1994) 306.

[70] K. Mohri, T. Uchiyama, P. V. Panina, *Recent advances of micro magnetic sensors and sensing application,* Sens. Actuators, A, 59 (1997) 1–8.

[71] S. Yabukami, H. Mawatari, N. Horikoshi, Y. Murayama, T. Ozawa, K. Ishiyama, et al., *A design of highly sensitive GMI sensor,* J. Magn. Magn. Mater., 290–291(2005) 1318.

[72] K. Nesteruk, M. Kuzminski, H. K. Lachowicz, Sen. Trans Mag., 65 (2006) 515.

[73] Y. Honkura, *Development of amorphous wire type MI sensors for automobile use,* J Magn Magn Mater, 249 (2002) 375.

[74] M. Tejedor, B. Hernando, M. L. Sanchez, V.M. Prida, M. Vazquez, *Magneto-impedance effect in amorphous ribbons for stress sensor application,* Sens. Actuators, A, 81 (2001) 98.

[75] A. F. Cobeno, A. Zhukov, J. M. Blanco, V. Larin, J. Gonzalez, *Magnetoelastic sensor based on GMI of amorphous microwire,* Sens. Actuators, A, 91 (2001) 95.

[76] P. Sarkar, R.K. Roy, A.K. Panda, A. Mitra, *Development of a GMI Sensor for Evaluating-Microstructural Degradation in Ferromagnetic Material*s, Inter. Conf. proceeding of IEEE Xplore, (2012) 108–111.

[77] V. Panina and K. Mohri, *Magneto-impedance effect in amorphous wires,* Appl. Phys. Lett., 65, (1994), 1189.

[78] T. Meydan, Application of amorphous materials to sensors, J. Magn. Magn. Mater., 133 (1994) 525–32.

IntechOpen